

# Speed control of multiphase cage induction motors incorporating supply sequence

PIOTR DROZDOWSKI

*Institute of Electromechanical Energy Conversion  
Cracow University of Technology  
Warszawska 24, 31-155 Kraków, Poland  
e-mail: xpiotrd@wp.pl, pdrozdow@pk.edu.pl*

(Received: 23.10.2013, revised: 05.05.2014)

**Abstract:** The subject of this paper is the control possibility of the multiphase cage induction motors having number of phases greater than 3. These motors have additional properties for speed control that distinguish them from the standard 3 phase motors: operation at various sequences of supplying voltages due to the inverter control and possible operation with few open-circuited phases. For each supply sequence different no load speeds at the same frequency can be obtained. This feature extends the motor application for miscellaneous drive demands including vector or scalar control. This depends mainly on the type of the stator winding for a given number of phases, since the principle of motor operation is based on co-operation of higher harmonics of magnetic field. Examples of operation are presented for a 9-phase motor, though general approach has been discussed. This motor was fed by a voltage source inverter at field oriented control with forced currents. The mathematical model of the motor was reduced to the form incorporating all most important physical features and appropriate for the control law formulation. The operation was illustrated for various supply sequences for “healthy” motor and for the motor operating at one phase broken. The obtained results have shown that parasitic influence of harmonic fields interaction has negligible influence on motor operation with respect to the useful coupling for properly designed stator winding.

**Key words:** multiphase cage induction motor, supply sequence, speed control, multiphase voltage source inverter, field oriented control

## 1. Introduction

The multiphase cage induction motors, with number of stator phases  $M > 3$ , have features distinguishing them from the standard 3-phase motors and allowing for specific control methods. The stator  $M$ -phase winding shown in Figure 1a has the number of pole pairs  $p = 1$  and is composed of short- or full-pitched groups of coils. This multiphase winding must be supplied by a multiphase voltage- or current source. Theoretically this can be the  $M$  phase system of sinusoidal voltages or currents. In practice the supplying device is a power electronics converter – the practically useful device is a voltage source inverter (VSI) – Figure 1b. It can

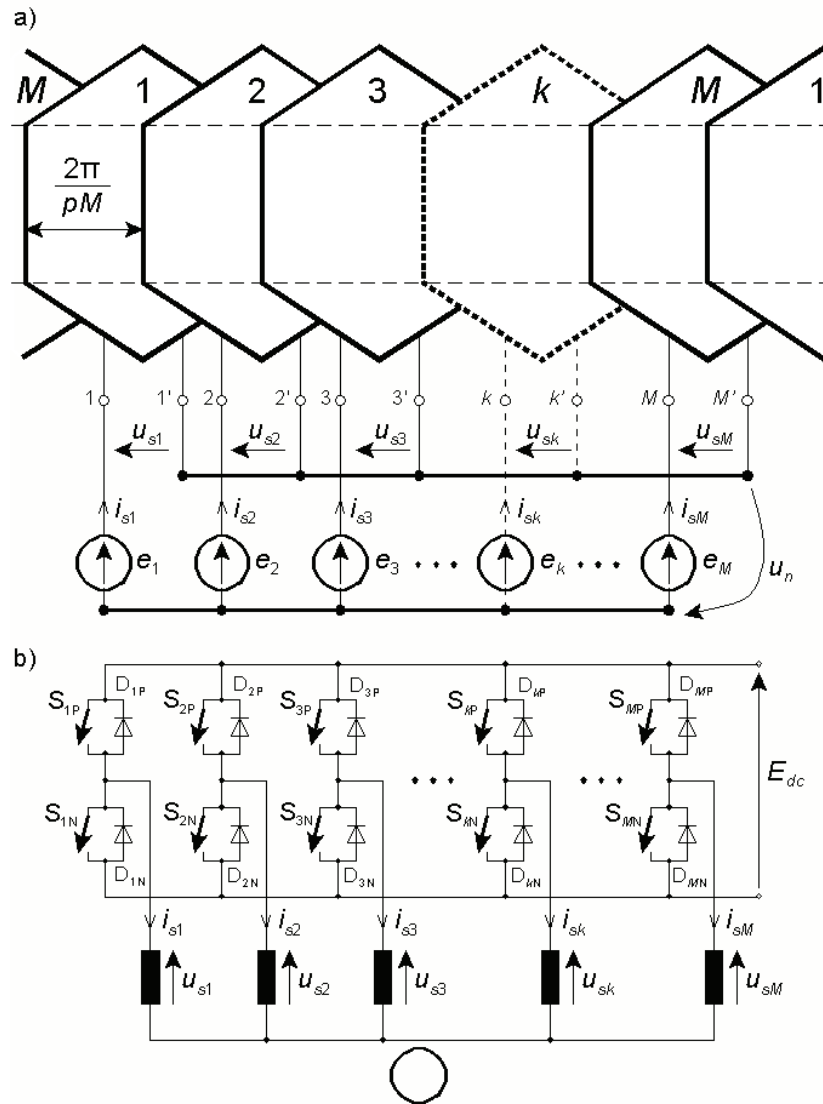


Fig. 1. Connection of an  $M$ -phase winding to an  $M$ -phase supply system, a) symbolic  $M$ -phase winding distribution and the supply system, b) voltage source inverter supplying the  $M$ -phase stator winding of the motor

operate at both modes as a voltage or a current source. The current source inverter has not been considered, though it offers other control possibilities for shaping the output voltages and currents.

Number of phases greater than 3 gives the possibility for supply with different sequences of voltages at a variable or a constant frequency. This can be explained using sinusoidal voltages (1) supplying  $M$  stator phase windings of the motor. The supply sequence is determined in (1) by numbers  $m = 0, 1, 2, 3, \dots, M - 1$ .

$$\mathbf{E}_{s1} = \begin{bmatrix} e_1 \\ e_2 \\ e_3 \\ e_4 \\ \vdots \\ e_M \end{bmatrix} = E_s \begin{bmatrix} \sin(\vartheta_s) \\ \sin(\vartheta_s - m \frac{2\pi}{M}) \\ \sin(\vartheta_s - 2m \frac{2\pi}{M}) \\ \sin(\vartheta_s - 3m \frac{2\pi}{M}) \\ \vdots \\ \sin[\vartheta_s - (M-1)m \frac{2\pi}{M}] \end{bmatrix} \quad m = 0, 1, 2, \dots, M-1 \quad (1)$$

$$\vartheta_s = 2\pi \int_0^t f_s(\tau) d\tau$$

Each  $m$  causes the other mutual phase shift of the voltages as a multiple of  $2\pi/M$ . So, the motor can be supplied with  $M$  different  $M$ -phase sets of symmetrical voltages having the same frequency and amplitude. The  $k$ -th voltage source  $e_k = E_s \sin[\vartheta_s - (k-1)m \cdot 2\pi/M]$  is connected to the  $k$ -th winding ( $k = 1, 2, \dots, M$ ).

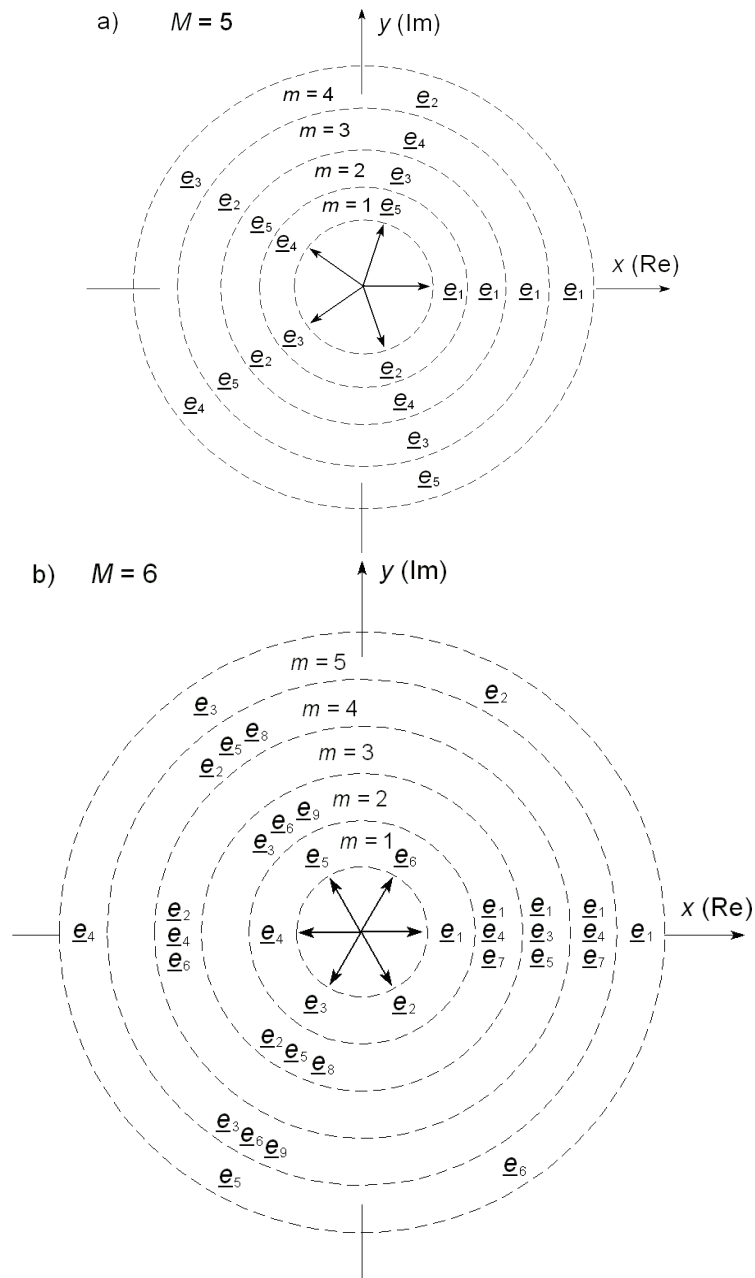
For example the 3-phase motor ( $M = 3$ ) can be supplied with 3 sequences  $m = 0, 1, 2$ . For  $m = 0$  all voltages  $e_1, e_2, e_3$  are in phase assuming the same value. This is so called “zero” sequence. For  $m = 1$  we obtain so called “positive” or “forward” 3-phase sequence and for  $m = 2$  the “negative” or “backward” sequence. Thus, we have 3 sets of 3-phase symmetrical systems that can supply a 3-phase winding, from which the last two sequences are only useful. They allow for both directions of the motor speed. For  $m > 3$  there are more sequences.

To illustrate the effect of phase shift between the phase voltages the star diagram of phasors representing voltages (1) in the reference frame ( $x - y$ ) rotating at the speed  $\omega_s = d\vartheta_s/dt$  is shown in Figure 2 for three numbers of phases. For every number  $m$  the phasors  $\underline{e}_1, \underline{e}_2, \dots, \underline{e}_M$  are shifted successively by the angle  $m \cdot 2\pi/M$  with respect to the preceding one. The real axis  $x$  coincides with the phasor  $\underline{e}_1$ . In this figure the phasors for so called forward sequences  $m = m_{(+)} = 1, 2, \dots, m_M$  and the so called backward sequences  $m = m_{(-)} = M - m_{(+)} = M - 1, M - 2, \dots, M - m_M$  have been depicted. The number  $m_M$  of forward or backward sequences is given below.

$$\left. \begin{aligned} m_M &= \frac{M-1}{2} \text{ for odd } M \\ m_M &= \frac{M-1}{2} \text{ for even } M \end{aligned} \right\} \quad (2)$$

The stars of phasors, shown in Figure 2, are symmetrical and the number of representing arrows is equal to  $M$ . At a given  $m$  the assignment of voltages  $\underline{e}_1, \underline{e}_2, \dots, \underline{e}_M$  to the respective phasor has been shown between the dashed circles. So, it means that the angle shift between voltages supplying subsequent stator phase windings is a multiplication  $m$  of  $2\pi/M$ . For example when  $M = 5$  the operation at the sequence  $m = 4$  is opposite to the operation at  $m = 1$ . The operation at  $m = 3$  is opposite to that with  $m = 2$ . The zero sequence phasor is only for  $m = 0$  and 5. The same rule can be observed for the next phase numbers  $M = 6$  and for  $M = 9$ .

For example at  $M = 6$  the sequence  $m = 3$  appears as two “zero sequences” supplying both the 3-phase windings constituting the 6-phase system, whereas for  $M = 9$  the sequence  $m = 3$  means that the motor operates as the 3-phase one with phase windings (1, 4, 7), (2, 5, 8) and (3, 6, 9) connected in parallel.



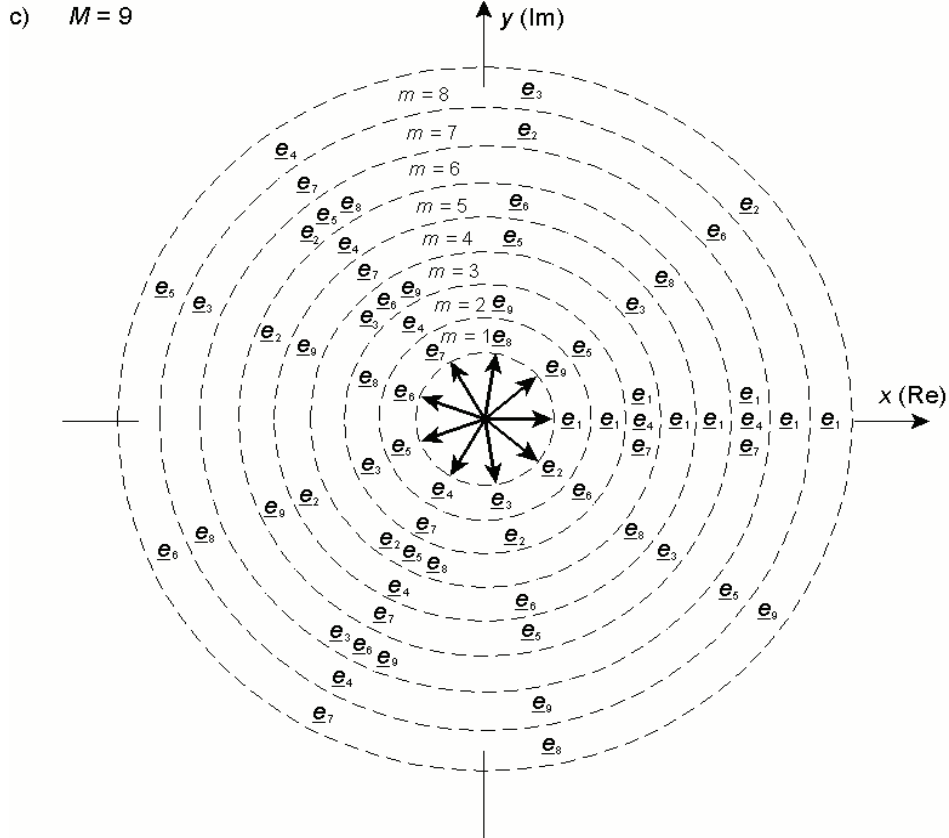


Fig. 2. The phasor stars of multiphase voltages for numbers of supply sequences  $m$  and number of phases: a)  $M = 5$ , b)  $M = 6$ , c)  $M = 9$

As it was defined in [8] the multiphase stator windings can be divided into two types. Both of the types differs each other with spatial harmonic orders of resultant magneto motive force (MMF):

$$\nu = 1, (2 - S)2, 3, (2 - S)4, 5, \dots \quad (3)$$

The number  $S$  assumes two values:  $S = 1$  indicates the winding of the first type, and  $S = 2$  is relevant to the second type winding. The winding of the first type produces MMF containing odd and even harmonics, whereas the winding of the second type only odd harmonics. This depends on the structure of the winding and is valid for every coil shape. For the first type winding the harmonic numbers are  $\nu = 1, 2, 3, 4, 5, \dots$ , whereas for the second type  $\nu = 1, 3, 5, 7, 9, \dots$ . The first  $M - 1$  harmonics are the most important.

Supplying the stator winding at the sequence  $m$  and the frequency  $f_s$  the main rotating field with the number of poles  $2mp$  is created [8], where  $p$  is the number of pole pairs specific for the winding design. Thus, different no load speeds of the motor can be obtained. The number of these speeds for one direction is given by  $m_M(2)$ . The forward sequences  $m = m_{(+)}$  give the

following no load speeds:

$$\Omega_{0(+)} = \frac{2\pi f_s}{p \cdot m_{(+)}}. \quad (4)$$

The backward sequences  $m = m_{(-)}$  give the opposite no load speeds:

$$\Omega_{0(-)} = \frac{2\pi f_s}{p \cdot (m_{(-)} - M)}. \quad (5)$$

Usually the multiphase winding should have  $p = 1$  to obtain the slot number per pole and phase not lower than 2.

When  $M$  is divisible by 3, then at the sequence number  $m = M/3$  the multiphase motor operates as the 3-phase one where the phase coils are connected in parallel (Fig. 2 for  $M = 6$  and  $M = 9$ ). E.g., the 6-phase motor can be considered as the 3-phase one with switched stator winding giving two numbers of poles for  $m = 1$  and  $m = 2$ .

Mechanical characteristics of the motor depend on the stator winding design. So, for the two types of them two different families of the characteristics can be obtained (Fig. 3). Every supply sequence, denoted by  $m$ , is responsible for the respective curve. All the characteristics in Figure 3a are given for the same frequency  $f_s$ , the same amplitude of supplying voltage and differing  $m$ . The characteristics in Figure 3b are also for the same frequency but for the voltage diminished proportionally to  $m$ . So, the characteristics from Figure 3a are suitable for the loading torque  $T_L$  assuring approximately constant mechanical power, whereas the characteristics from Figure 3b are better for the fan type loading. The points between the curves are available due to the control of supplying voltage and frequency.

When the multiphase motor has sinusoidal distribution of phase windings, it can operate only at  $m = 1$  and  $m = M - 1$ . Such a winding does not produce higher harmonics of the magnetic field and number of poles is always  $2p$  independently of the supply sequence. The no load speed is then:

$$\Omega_0 = \pm \frac{2\pi f_s}{p}.$$

The work at different sequences and regulated frequency gives new possibilities for vector, scalar or direct torque control. Lower speeds for the motor with the stator winding of the first type ( $S = 1$ ) can be obtained by increasing  $m$  at constant frequency  $f_s$  and voltage  $U_s$ . For example the 9-phase motor ( $S = 1$ ) has the greatest no load speed  $\Omega_{0(+1)}$  for  $m = 1$ . For  $m = 4$  the no load speed is four times lower  $\Omega_{0(+4)} = \Omega_{0(+1)}/4$ . Similarly, the 9-phase motor with the second type winding ( $S = 2$ ) can reach even a lower speed  $\Omega_{0(+7)} = \Omega_{0(+1)}/7$  for  $m = 7$  and the same frequency as for  $m = 1$ . However, the amplitude of voltage must be regulated for this kind of winding. The voltage must be diminished practically seven times to set the magnetising current on the adequately low level. For the first type winding this current is proportional to  $m^{0.5}$  and for the second type it is proportional to  $m^2$  [10]. This explains the shapes of the mechanical characteristics in Figure 3. The curve for  $m = 7$  has not been shown in Figure 3b as practically usefulness.

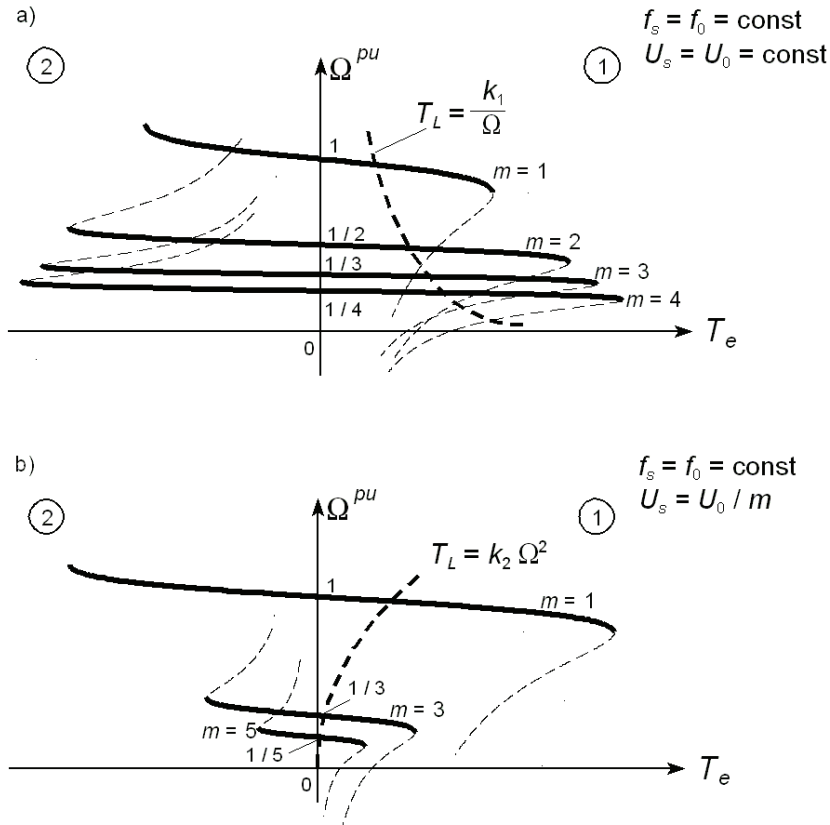


Fig. 3. Typical mechanical characteristics of multiphase motors for two types of stator winding:  
 a)  $S=1$ , b)  $S=2$

The described practical applications of the multiphase induction motors e.g. [1, 2, 18, 19, 22, 24, 28, 30] were limited in most to the motors with 5 and 7 stator phases having only the stator winding of the second type ( $S=2$ ) and operating only at  $m=1$ . There were considered sinusoidally distributed winding or concentrated windings with symmetrical poles. Here must be noticed that the short-pitched concentrated windings with asymmetrical poles belong to the mentioned above the first type windings ( $S=1$ ). However, this case has not been analysed in the cited papers. The mathematical models of the multiphase machines take into account only the first few higher harmonics of MMF [14, 18, 22] for the machines with concentrated windings and a concrete number of rotor cage bars [22]. So, some phenomena connected with parasitic interaction of space harmonics and the supply harmonics cannot be considered. The generalised approach, taking into account the mutual influence of number of phases  $M$ , MMF harmonics, the stator winding- and the rotor design, was presented in [10].

As it was mentioned above the multiphase windings of the second type ( $S=2$ ) are disadvantageous for control with variable supply sequence, since regulation of supplying voltage with respect to the sequence number  $m$  is necessary. However for operation with one chosen

sequence the winding can be designed optimally to obtain, e. g. the greatest torque at the lowest energy consumption. This case is met by the sinusoidal windings designed to operate at the first supply sequence [1, 2, 18, 19, 24]. The design experience of the 3-phase induction machines can be applied then to the  $M$ -phase motors.

Historically, the influence of supply with two voltage sequences was analysed in early paper [23] for the 5-phase motor. This change of sequence was realised there by winding switching. The 3-phase induction motor with switchable Dahlander's winding can be considered as the 6-phase motor with switched supply sequence (Fig. 2b). The so called dual 3-phase induction motor, with two sets of three phase stator windings spatially shifted by  $30^\circ(\text{el.})$  [19], cannot be regarded as a 6-phase motor and it can operate only at the sequence  $m = 1$ . The first approach to the switching between mechanical characteristics due to change of voltage supply sequence of the 7-phase motor was published in [26]. The motor had there the stator winding of the first type ( $S = 1$ ).

Comparing the multiphase motor to the 3-phase one the difference appears in possible work of the multiphase motor with a few open-circuited phases. The 3-phase motors connected to the three-phase source can operate only at  $m = 1$  and  $m = 2$  for both speed directions. The break in a phase after motor starting causes switching off the motor. The multiphase motor with such a damage has a starting torque and can operate under frequency control. Such damages can be caused by breaks in the supply system (e.g. a damage of inverter) or by open-circuited motor phases [1, 6, 7, 10, 11, 15, 30].

In this paper the principle of vector control specified for the multiphase motors operating in variable speed drives is presented. It was initially presented in [13]. The formula describing the electromagnetic torque was simplified to the case of sinusoidal winding with the fundamental MMF harmonic  $\nu = m$  for a given supply sequence  $m$ . Thus, the control system structure was based on this simplified model. However, this control was applied to the drive model where the multiphase motor was represented by the mathematical model pretending the real machine with interaction of higher harmonics of magnetic fields.

The multiphase motors have found application in locomotive traction [11, 12, 20, 27], electric ship propulsion [16, 29] and the aircraft equipment [3]. However, the motors can be more attractive for traction drives and electrical cars since the switched supply sequence gives a similar effect as the switched mechanical gear-box for the loading torque. However, the supply sequence does not change the moment of inertia reduced to the motor shaft as it occurs with the real gear-box.

## 2. Reduced mathematical model and principle of control

The set of equations describing the multiphase motor in natural variables has a typical form for the circuit composed of resistances and inductances representing this machine:

$$\begin{bmatrix} \mathbf{U}_{s1} \\ \mathbf{0} \end{bmatrix} = \begin{bmatrix} \mathbf{R}_{s1} & \\ & \mathbf{R}_{r1} \end{bmatrix} \begin{bmatrix} \mathbf{I}_{s1} \\ \mathbf{I}_{r1} \end{bmatrix} + \frac{d}{dt} \begin{bmatrix} \mathbf{L}_{s1} & \mathbf{M}_{sr1} \\ \mathbf{M}_{sr1}^T & \mathbf{L}_{r1} \end{bmatrix} \begin{bmatrix} \mathbf{I}_{s1} \\ \mathbf{I}_{r1} \end{bmatrix}. \quad (6)$$



These equations must be supplemented with the simplest mechanical equation at least:

$$J \frac{d\omega}{dt} = T_e - T_L. \quad (7)$$

Electromagnetic torque takes the form as for all electrical machines:

$$T_e = \mathbf{I}_{s1}^T \frac{\partial}{\partial \varphi} \mathbf{M}_{sr1} \mathbf{I}_{r1}. \quad (8)$$

Vectors of stator phase voltages  $\mathbf{U}_{s1}$  and the phase currents  $\mathbf{I}_{s1}$  have the same dimension  $M$ . Vector of rotor currents  $\mathbf{I}_{r1}$  has dimension  $N$  equal to number of rotor cage meshes treated as shorted rotor phases. The matrices of stator resistances  $\mathbf{R}_{s1}$  and leakage inductances  $\mathbf{L}_{\sigma s1}$  are usually diagonal (when neglecting mutual coupling between phases due to leakage fluxes). The matrix of rotor resistances  $\mathbf{R}_{r1}$  and the matrix  $\mathbf{L}_{\sigma r1}$  of rotor leakage inductances incorporate self and mutual elements among adjacent cage meshes. The matrices of leakage inductances are included into main stator and rotor inductances  $\mathbf{L}_{s1}$  and  $\mathbf{L}_{r1}$ . The most important is matrix  $\mathbf{M}_{sr1}$  of mutual inductances between stator and rotor circuits, since main features of the motor are coded in this matrix depending on the rotor rotation angle  $\varphi$ . Every self and mutual inductance in  $\mathbf{M}_{sr1}$  is a sum of harmonic inductances depending on number of field harmonics taken for account. Parameters of such a model were developed and published in [10].

The transformation to symmetrical components, separately for the stator and the rotor vectors, gives two profits: the natural variables become space vectors represented by appropriate symmetrical components and the set of equations takes a useful structure allowing for the control law. This transformation acts as a kind of mathematical filter separating equivalent circuits for groups of harmonics and allowing for transformation to rotating reference frames.

The transformation matrix for the stator and rotor variables takes the following form:

$$\mathbf{C}_X = \frac{1}{\sqrt{X}} \begin{bmatrix} 1 & 1 & 1 & \dots & 1 \\ 1 & \underline{a} & \underline{a}^2 & \dots & \underline{a}^{X-1} \\ 1 & \underline{a}^2 & \underline{a}^4 & \dots & \underline{a}^{2(X-1)} \\ \vdots & \vdots & \vdots & \ddots & \vdots \\ 1 & \underline{a}^{X-1} & \underline{a}^{2(X-1)} & \dots & \underline{a}^{(X-1)^2} \end{bmatrix}, \quad (9)$$

$$\underline{a} = e^{j \frac{2\pi}{X}},$$

$X = M$  for the stator and  $X = N$  for the rotor.

After this transformation the vector of stator voltages takes the form:

$$\mathbf{U}_{s2} = \mathbf{C}_M \mathbf{U}_{s1} = \left[ \underline{u}_s^{(0)} - \sqrt{M} u_n, \underline{u}_s^{(1)}, \underline{u}_s^{(2)}, \dots, \underline{u}_s^{(W)}, \dots, \underline{u}_s^{(M-W)}, \dots, \underline{u}_s^{(M-2)}, \underline{u}_s^{(M-1)} \right]^T. \quad (10)$$

Similarly is for the vector of stator currents  $\mathbf{I}_{s2}$ . The symmetrical components  $\underline{u}_s^{(W)}$  and  $\underline{u}_s^{(M-W)}$  are conjugate, whereas  $u_n$  is the neutral voltage between the star point of the supply and the point of the stator winding (Fig. 1). If the supplying voltages are sinusoidal (1), then

$$\mathbf{U}_{s2} = \frac{\sqrt{M}}{2j} E_s \left\{ \begin{array}{c} \left[ \begin{array}{c} 0 \\ 0 \\ \vdots \\ c^{(W)} \\ \vdots \\ 0 \\ \vdots \\ 0 \end{array} \right] e^{j\theta_s} - \left[ \begin{array}{c} 0 \\ 0 \\ \vdots \\ 0 \\ \vdots \\ c^{(W)} \\ \vdots \\ 0 \end{array} \right] e^{-j\theta_s} \end{array} \right\}, \quad (11)$$

$$\left. \begin{array}{l} c^{(W)} = 1 \text{ for } W = m \\ c^{(W)} = 0 \text{ for } W \neq m \end{array} \right\}. \quad (12)$$

After the transformation to symmetrical components the motor equations have the following form:

$$\begin{bmatrix} \mathbf{U}_{s2} \\ \mathbf{0} \end{bmatrix} = \begin{bmatrix} \mathbf{R}_{s2} & \\ & \mathbf{R}_{r2} \end{bmatrix} \begin{bmatrix} \mathbf{I}_{s2} \\ \mathbf{I}_{r2} \end{bmatrix} + \begin{bmatrix} \mathbf{L}_{s2} & \\ & \mathbf{L}_{r2} \end{bmatrix} \frac{d}{dt} \begin{bmatrix} \mathbf{I}_{s2} \\ \mathbf{I}_{r2} \end{bmatrix} + \frac{d}{dt} \begin{bmatrix} \mathbf{0} & \mathbf{M}_{sr2} \\ \mathbf{M}_{sr2}^T & \mathbf{0} \end{bmatrix} \begin{bmatrix} \mathbf{I}_{s2} \\ \mathbf{I}_{r2} \end{bmatrix}. \quad (13)$$

The matrices  $\mathbf{R}_{s2}$ ,  $\mathbf{R}_{r2}$ ,  $\mathbf{L}_{s2}$ ,  $\mathbf{L}_{r2}$  are diagonal. The dimension of matrix  $\mathbf{M}_{sr2}$  is  $M \times N$  and this matrix is generally fulfilled. Its parameters are dependent on the rotor rotation angle  $\varphi$ . Each element of this matrix lying in row  $W$  and column  $K$  depends on the set of field harmonic orders  $H_{WK}$  relevant to this strictly determined place. Because of Euler's identity the set  $H_{WK}$  contains positive and negative numbers  $\nu$ . Thus, for all harmonics appreciating the MMF the same amount of positive and negative harmonics must be considered. So, the mutual inductance is described by the formula:

$$\underline{M}_{WK}^{sr} = \sum_{\nu \in H_{WK}} M_{\nu}^{sr} e^{j\nu p \varphi}; \quad W = 0, 1, \dots, M-1; \quad K = 0, 1, \dots, N-1. \quad (14)$$

The coefficient  $M_{\nu}^{sr}$  depends on the stator inside diameter  $d_c$ , magnetic core length  $l_c$ , air-gap length  $\delta$ , number of stator phase turns  $N_s$ , and winding factors: for the stator

$k_s^{|\nu|}$  and for the rotor  $k_r^{|\nu|}$ . The skew factor  $k_{sk}^{|\nu|}$  is also taken into account.

$$M_{\nu}^{sr} = \sqrt{MN} \frac{\mu_0 d_c l_c}{\pi \delta} N_s \frac{k_s^{|\nu|} k_r^{|\nu|} k_{sk}^{|\nu|}}{(\nu p)^2}. \quad (15)$$

To formulate matrix  $\mathbf{M}_{sr2}$  a table of relevant harmonic orders is sufficient. For the 9-phase motor this table has been shown below as an example. For simplicity only the lowest harmonic orders belonging to  $H_{WK}$  are presented there. They are the most important. In spite of that the matrix has 251 non-zero elements. Main features of the multiphase motor depend on dominant harmonics depicted in dark patches of the table.

When the motor is supplied with sinusoidal voltages at a sequence  $m$ , the voltage vector (11) of symmetrical components has only two non-zero elements in rows  $W = m$  and  $M - W = M - m$  (12).

Table 1. Table of harmonics for  $M = 9, N = 28, S = 1, p = 1$ 

$W \setminus K$	0	1	2	3	4	5	6	7	8	9	10	11	12	13	14
0	-	-27	-54	-81	-108	117	90	63	36	9	-18	-45	-72	-99	-
1	28	1	-26	-53	-80	-107	118	91	64	37	10	-17	-44	-71	-98
2	56	29	2	-25	-52	-79	-106	119	92	65	38	11	-16	-43	-70
3	84	57	30	3	-24	-51	-78	-105	120	93	66	39	12	-15	-42
4	112	85	58	31	4	-23	-50	-77	-104	121	94	67	40	13	-14
5	-112	113	86	59	32	5	-22	-49	-76	-103	122	95	68	41	14
6	-84	-111	114	87	60	33	6	-21	-48	-75	-102	123	96	69	42
7	-56	-83	-110	115	88	61	34	7	-20	-47	-74	-101	124	97	70
8	-28	-55	-82	-109	116	89	62	35	8	-19	-46	-73	-100	125	98

$W \setminus K$	15	16	17	18	19	20	21	22	23	24	25	26	27
0	99	72	45	18	-9	-36	-63	-90	-117	108	81	54	27
1	-125	100	73	46	19	-8	-35	-62	-89	-116	109	82	55
2	-97	-124	101	74	47	20	-7	-34	-61	-88	-115	110	83
3	-69	-96	-123	102	75	48	21	-6	-33	-60	-87	-114	111
4	-41	-68	-95	-122	103	76	49	22	-5	-32	-59	-86	-113
5	-13	-40	-67	-94	-121	104	77	50	23	-4	-31	-58	-85
6	15	-12	-39	-66	-93	-120	105	78	51	24	-3	-30	-57
7	43	16	-11	-38	-65	-92	-119	106	79	52	25	-2	-29
8	71	44	17	-10	-37	-64	-91	-118	107	80	53	26	-1

This means that only two stator equations, mutually conjugated, are forced with non-zero voltages. The remaining are supplied with a zero voltage together with the rotor equations. It means these equivalent circuits are shorted and they are supplied due to magnetic coupling. Analysing the example presented in Table 1 it is visible that non-zero supplying voltages for all sequence numbers  $m$  are in rows  $W = m = 1, 2, 3, 4, 5, 6, 7, 8$  for which the space harmonics  $v = (1, 10, -8)_{m=1}, (2, 11, -7)_{m=2}, (3, 12, -6)_{m=3}, (4, 13, -5)_{m=4}, (5, -13, -4)_{m=5}, (6, -12, -3)_{m=6}, (7, -11, -2)_{m=7}, (8, -10, -1)_{m=8}$  are the dominant. This analysis leads to the conclusion that the most important harmonics for a given supply sequence  $m$  are for  $v = \pm m, \pm(m - S \cdot M), \pm(m + S \cdot M)$ . They have the lowest numbers and cause the strongest magnetic coupling  $M_v^{\sigma}$  (15) producing the greatest electromagnetic torque components. Among them are fundamental harmonics  $v = \pm m$  decisive for the no load speeds (4), (5) of the motor. Harmonic orders  $v = \pm(m - S \cdot M), \pm(m + S \cdot M)$  are responsible for main parasitic rotating fields and additionally for the parasitic torque components. For specifically designed stator winding their influence can be significantly suppressed [8]. Going on there are also motors that can not start in rush at some sequence  $m$  and at any frequency  $f_s$  because of interaction of higher field harmonics producing asynchronous torques. Such a real case was presented in [10].

The voltage vector (11) empowers to simplify the mathematical model by selection two stator equations for non-zero  $\underline{u}_s^{(W)}$  and  $\underline{u}_s^{(M-W)}$  ( $W = m$ ) and omitting those for zero voltage. However, only equation for  $\underline{u}_s^{(W)}$  is sufficient, since both the equations are conjugated and they carry the same information. Hence, the reduced mathematical model for sinusoidal multiphase supply assumes the same form as for the mono harmonic 3-phase cage motor described in the stationary reference frame ( $\alpha$ - $\beta$ ):

$$\begin{bmatrix} \underline{u}_s^{(m)} \\ 0 \end{bmatrix} = \begin{bmatrix} R_s & \\ & R_r^{(m)} \end{bmatrix} \begin{bmatrix} \underline{i}_s^{(m)} \\ \underline{i}_r^{(m)} \end{bmatrix} + \frac{d}{dt} \begin{bmatrix} \underline{\psi}_s^{(m)} \\ \underline{\psi}_r^{(m)} \end{bmatrix} - j m p \omega \begin{bmatrix} \underline{\psi}_s^{(m)} \\ \underline{\psi}_r^{(m)} \end{bmatrix}. \quad (16)$$

Flux vectors and inductances of the model:

$$\begin{bmatrix} \underline{\psi}_s^{(m)} \\ \underline{\psi}_r^{(m)} \end{bmatrix} = \begin{bmatrix} L_s^{(m)} & L_\mu^{(m)} \\ L_\mu^{(m)} & L_r^{(m)} \end{bmatrix} \begin{bmatrix} \underline{i}_s^{(m)} \\ \underline{i}_r^{(m)} \end{bmatrix}, \quad (17)$$

$$L_s^{(m)} = L_{\sigma s} + L_\mu^{(m)}; \quad L_r^{(m)} = L_{\sigma r}^{(m)} + L_\mu^{(m)}$$

$$L_\mu^{(m)} = M_m^{sr} \xi_m; \quad \xi_m = \sqrt{\frac{M}{N}} N_s \frac{k_s^{|m|}}{k_r^{|m|} k_{sk}^{|m|}}. \quad (18)$$

The formula describing the electromagnetic torque depends on space vectors of stator and rotor currents:

$$T_e = 2 m p L_\mu^{(m)} \text{Im} \left\{ \underline{i}_s^{(m)} \underline{i}_r^{(m)*} \right\}. \quad (19)$$

For the above simplified model:  $m = m_{(+)} = 1, 2, \dots, m_M$  or  $m = m_{(-)} + M = -m_{(+)}$ . So,  $m = m_{(+)}$  gives the forward speeds and  $m = -m_{(+)}$  gives the backward speeds.

The spectrum of spatial harmonics (2) can be limited to the maximum number  $v_{\max} = m_M$ . The equations have now the same structure as equations describing the monoharmonic induction motor with the number of pairs of magnetic poles equal to  $mp$  instead of  $p$ .

All known control methods can be applied here for operation at a given sequence number  $m$ . However, it must be noticed that some model parameters (main inductance and rotor parameters) change their values with respect to  $m$  and the actual motor is influenced with harmonic fields interaction.

Transformation of the variables to the reference frame ( $d^{(m)} - q^{(m)}$ ), attached to the rotor flux vector  $\underline{\psi}_r^{(m)}$ , means that for every  $m$  individual transformation must be performed (Fig. 4). For this reference frame the electromagnetic torque takes the following form:

$$T_e = 2 m p \frac{L_\mu^{(m)}}{L_{\sigma r}^{(m)} + L_\mu^{(m)}} \text{Im} \left\{ \underline{i}_s^{(m)} \underline{\psi}_r^{(m)*} \right\} = 2 p m \frac{L_\mu^{(m)}}{L_{\sigma r}^{(m)} + L_\mu^{(m)}} \psi_r^{(m)} i_{sq}^{(m)}. \quad (20)$$

This expression indicates the control law of the multiphase motor. It means that for each  $m$  the rotor flux vector and the position  $\mathcal{G}^{(m)}$  of the ( $d^{(m)} - q^{(m)}$ ) reference frame must be determined separately. Parameters of flux controller must be adapted to  $m$ . Keeping the product

$\psi_r^{(m)} i_{sq}^{(m)}$  constant independently of  $m$  it allows for operation with a greater torque  $T_e$  at a lower speed  $\omega$  for increasing  $m$ . The motor can work with a constant power at wide range of speed (Fig. 3a).

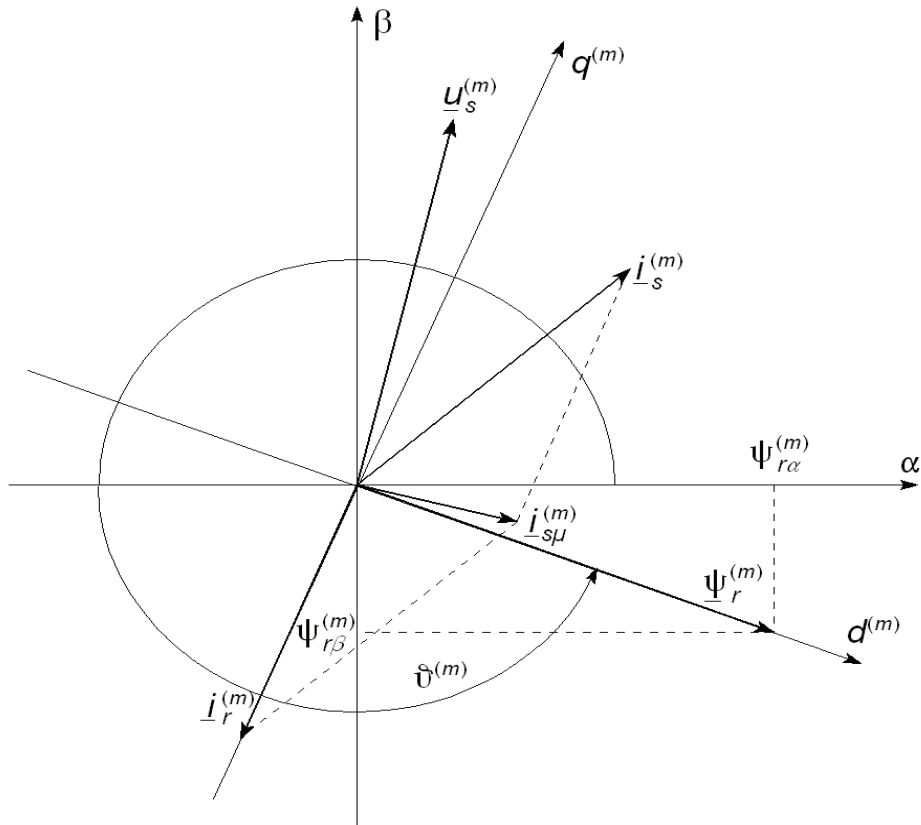


Fig. 4. Vectors in the stationary reference frame ( $\alpha$ - $\beta$ ) and in the individual reference frame ( $d^{(m)} - q^{(m)}$ ) for a given supply sequence number  $m$

In practice the multiphase motor is not supplied sinusoidally, e.g. from the VSI. The voltage vector takes the form:

$$\mathbf{U}_{s2} = \frac{\sqrt{M}}{2j} \sum_{\kappa \in H_\kappa} E_{s,\kappa} \left\{ \begin{array}{c} \begin{bmatrix} 0 \\ 0 \\ \vdots \\ c_\kappa^{(W)} \\ \vdots \\ 0 \\ \vdots \\ 0 \end{bmatrix} e^{j\kappa\theta_s} - \begin{bmatrix} 0 \\ 0 \\ \vdots \\ 0 \\ \vdots \\ c_\kappa^{(W)} \\ \vdots \\ 0 \end{bmatrix} e^{-j\kappa\theta_s} \end{array} \right\}. \quad (21)$$

In the above:  $\kappa$  – harmonic order of the supplying voltage belonging to the set  $H_\kappa = \{\pm(2n-1); n = 1, 2, \dots\}$ ,  $E_{s,\kappa}$  – voltage amplitude for harmonic order  $\kappa$ ,  $\vartheta_s$  – phase argument as for (1).  $\kappa^{\text{th}}$  time harmonics result from a “nature” of supplying unit or can be injected specifically to influence the machine.

$$\left. \begin{aligned} c_\kappa^{(W)} &= 1 \quad \text{for } W = (\kappa m) \bmod M = 0, 1, 2, \dots, M-1 \\ c_\kappa^{(W)} &= 0 \quad \text{otherwise} \end{aligned} \right\}. \quad (22)$$

Expression (21) indicates that all symmetrical components of non-sinusoidal supplying voltages are non-zero. The fundamental harmonic for  $\kappa = 1$  is dominant. In contradiction to sinusoidal supply the remaining symmetrical components for  $W \neq m$  excite additional current components. For example, applying additional harmonic  $\kappa = 3$  for a 5-phase motor ( $M = 5$ ) at the supply sequence  $m = 1$  causes a strong magnetic field component of sequence  $\kappa m = 3$  rotating in opposite direction with a half of the no load speed as for  $m = 1$  – see Equations (4) and (5). This third harmonic is profitable for the 3-phase motor fed by a VSI, whereas for the 5-phase one is injurious. However, injection of the opposite third harmonic  $\kappa = -3$  gives the similar strong field component of sequence  $M + \kappa \cdot m = 2$  rotating in the same direction as the field component for  $m = 1$ . So, it supports the fundamental field enlarging the electromagnetic torque of the motor. The motor operates then as supplied with the first- and the second sequence together. The injection of harmonic current components can be considered similarly for the motors with other number of phases. The harmonics of order  $\kappa = k \cdot M / m$ ,  $k = 1, 2, \dots$  cause zero sequence symmetrical components of supplying voltages. It must be noticed here that the interaction between the time and space harmonics is determined by magnetic coupling between circuits for all stator and rotor symmetrical components expressed by the stator-rotor matrix  $\mathbf{M}_{sr2}$ . The higher harmonics of supplying voltages cause electrical coupling between equations for all symmetrical components. The motor should be designed to assure the strongest magnetic coupling for space harmonics  $v = m_{(+)}$ . Hence, the sinusoidal PWM for the sequence number  $m = m_{(+)}$  justifies the simplified model for the drive control law.

### 3. Control system and drive operation

#### 3.1. Description of the control system

Similarly as for the 3-phase motors, the field oriented control of the multiphase motor can be performed using current or voltage control. The structure of the control system in the rotor flux oriented reference frame ( $d^{(m)}-q^{(m)}$ ) results from Equations (16) – (20). The difference between the 3-phase motor and the  $M$ -phase one appears only in adaptation to the sequence control and the operation at open-circuited phases. For the control with forced phase currents the structural scheme is presented in Figure 5. There are two main reference signals:  $\omega^{\text{ref}}$  – speed and  $\psi^{\text{ref}}$  – rotor flux. The control parameter is number  $m$  of the supply sequence. The system has two main controllers:  $\mathbf{R}\omega$  – speed controller (usually PI or P type with saturation),  $\mathbf{R}\psi$  – flux controller (usually PI type). The output signals:  $i_{sq}^{(m)\text{ref}}$  – command current controlling the torque,  $i_{sd}^{(m)\text{ref}}$  – command current controlling the flux, are transformed in blocs  $\mathbf{T1}$

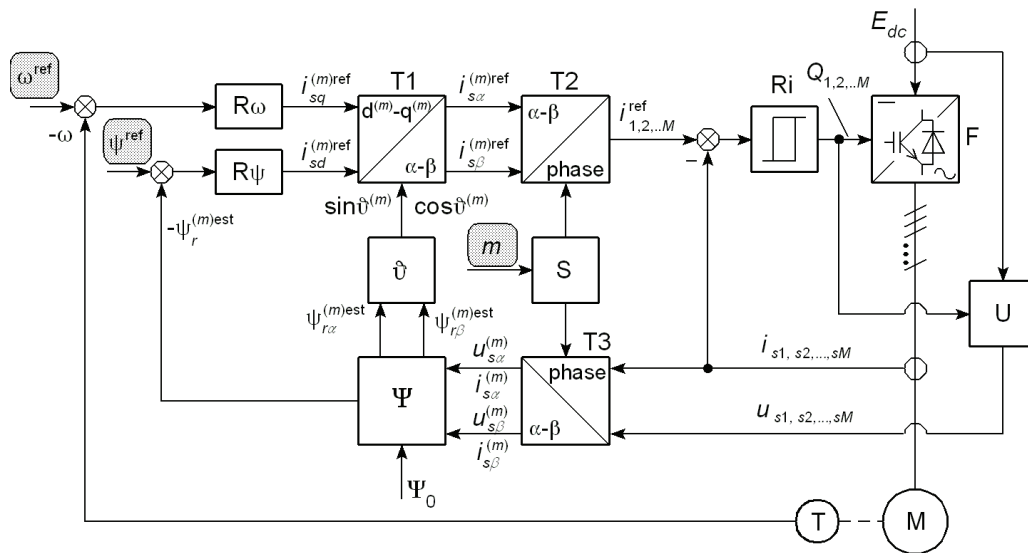


Fig. 5. Control scheme for the multiphase induction motor drive operating with forced currents under field oriented control with respect to rotor flux vector

and **T2** to the reference signals of phase currents  $i_{1,2,\dots,M}^{\text{ref}}$ . These signals are compared with the phase current signals in on-off controllers **Ri** of all half bridges of the  $M$ -phase voltage source inverter **F** (Fig. 1b). In the outputs the signals  $Q_1, Q_2, \dots, Q_k, \dots, Q_M$  of values +1 or -1 are produced. The signal  $Q_k = 1$  turns on the switch  $S_{kP}$  of a half-bridge and turns off  $S_{kN}$ . For  $Q_k = -1$  is vice versa. Block **Ψ** is the flux estimator and block **ϑ** determines position  $\vartheta^{(m)}$  of the rotor flux vector for the sequence number  $m$ . Block **S** selects  $m$ -th symmetrical component of voltages and currents eliminating the remaining, even if they are not equal to zero. Stator phase voltages  $u_{sk}$  are calculated in block **U** to avoid errors caused by voltage sensors during measurements of alternating signals (e.g. a dc component due to the voltage drift):

$$u_{sk} = \frac{E_{dc}}{2} \left( Q_k - \frac{1}{M} \sum_{l=1}^M Q_l \right)_{|k=1,2,\dots,M}, \quad (23)$$

where  $E_{dc}$  is the measured dc-link voltage.

Block **T1** realises the following operation:

$$\begin{bmatrix} i_{s\alpha}^{(m)\text{ref}} \\ i_{s\beta}^{(m)\text{ref}} \end{bmatrix} = \begin{bmatrix} \cos \vartheta^{(m)} & -\sin \vartheta^{(m)} \\ \sin \vartheta^{(m)} & \cos \vartheta^{(m)} \end{bmatrix} \begin{bmatrix} i_{sd}^{(m)\text{ref}} \\ i_{sq}^{(m)\text{ref}} \end{bmatrix}. \quad (24)$$

Blocks **T2** and **T3** realise mutually reverse operations. This is the transformation from phase quantities to  $\alpha$ - $\beta$  components or vice versa. Additionally, selection of the components appropriate for the sequence  $m$  is superimposed on this transformation. The remaining com-

ponents are eliminated since they are not useful for control even if they are not equal to zero. This selection is performed in block **S**.

The transformation of phase currents and phase voltages to the  $\alpha$ - $\beta$  components in **T3** is described by the following formula:

$$\left[ x_{s\alpha}^{(1)}, x_{s\alpha}^{(2)}, \dots, x_{s\alpha}^{(n)}, \dots, x_{s\beta}^{(n)}, \dots, x_{s\beta}^{(2)}, x_{s\beta}^{(1)} \right]^T = \mathbf{K}_{\text{ph}}^{\alpha\beta} \left[ x_{s1}, x_{s2}, \dots, x_{sM} \right]^T. \quad (25)$$

The variables  $x_{s1}, x_{s2}, \dots, x_{sM}$  mean phase currents or voltages where instead of  $x$  the letters  $i$  or  $u$  exist for currents and voltages respectively.

The transformation matrix  $\mathbf{K}_{\text{ph}}^{\alpha\beta}$  is a product of two matrices:  $\mathbf{J}_S$  – decomposition matrix and  $\mathbf{C}_{(M-1) \times M}$  – matrix of transformation to symmetrical components (9) without the row for zero component. Thus, this matrix is described by the expression:

$$\mathbf{K}_{\text{ph}}^{\alpha\beta} = \mathbf{J}_S \mathbf{C}_{(M-1) \times M} = \frac{1}{2\sqrt{M}} \begin{bmatrix} 1 & \dots & 1 \\ & 1 & \dots & 1 \\ & & 1 & \dots & 1 \\ \vdots & \vdots & \vdots & \ddots & \vdots \\ & & -j & \dots & j \\ & -j & \dots & & j \\ -j & & \dots & & j \end{bmatrix} \begin{bmatrix} 1 & \underline{a} & \underline{a}^2 & \dots & \underline{a}^{M-1} \\ 1 & \underline{a}^2 & \underline{a}^4 & \dots & \underline{a}^{2(M-1)} \\ \vdots & \vdots & \vdots & \ddots & \vdots \\ 1 & \underline{a}^{M-1} & \underline{a}^{2(M-1)} & \dots & \underline{a}^{(M-1)^2} \end{bmatrix}. \quad (26)$$

The inverse transformation takes the form:

$$\mathbf{K}_{\alpha\beta}^{\text{ph}} = 2 \mathbf{K}_{\text{ph}}^{\alpha\beta T}. \quad (27)$$

Block **S** contains the coefficients

$$S_n = \begin{cases} 1 & \text{for } n = m \\ 0 & \text{for } n \neq m \end{cases} \quad (28)$$

selecting voltage and current components according to the following formula (block **T3**):

$$x_{s\alpha,\beta}^{(m)} = \left[ S_1, S_2, \dots, S_n, \dots, S_{mM}, S_{(M-mM)}, \dots, S_{(M-n)}, \dots, S_{(M-2)}, S_{(M-1)} \right] \begin{bmatrix} x_{s\alpha,\beta}^{(1)} \\ x_{s\alpha,\beta}^{(2)} \\ \vdots \\ x_{s\alpha,\beta}^{(n)} \\ \vdots \\ x_{s\alpha,\beta}^{(mM)} \\ x_{s\alpha,\beta}^{(M-mM)} \\ \vdots \\ x_{s\alpha,\beta}^{(M-n)} \\ \vdots \\ x_{s\alpha,\beta}^{(M-2)} \\ x_{s\alpha,\beta}^{(M-1)} \end{bmatrix}. \quad (29)$$



In the above the following is valid

$$x_{s\alpha}^{(n)} = x_{s\alpha}^{(M-n)} ; x_{s\beta}^{(n)} = -x_{s\beta}^{(M-n)}. \quad (30)$$

Hence, we obtain the signals of current command values

$$\begin{bmatrix} i_1^{\text{ref}} \\ i_2^{\text{ref}} \\ i_3^{\text{ref}} \\ \vdots \\ i_4^{\text{ref}} \end{bmatrix} = \mathbf{K}_{\alpha\beta}^{\text{ph}} \begin{bmatrix} S_1 + S_{M-1} & 0 \\ S_2 + S_{M-2} & 0 \\ \vdots & \vdots \\ S_{m_M} + S_{M-m_M} & 0 \\ 0 & S_{m_M} - S_{M-m_M} \\ \vdots & 0 \\ 0 & S_2 - S_{M-2} \\ 0 & S_1 - S_{M-1} \end{bmatrix} \begin{bmatrix} i_{s\alpha}^{(m)\text{ref}} \\ i_{s\beta}^{(m)\text{ref}} \end{bmatrix}. \quad (31)$$

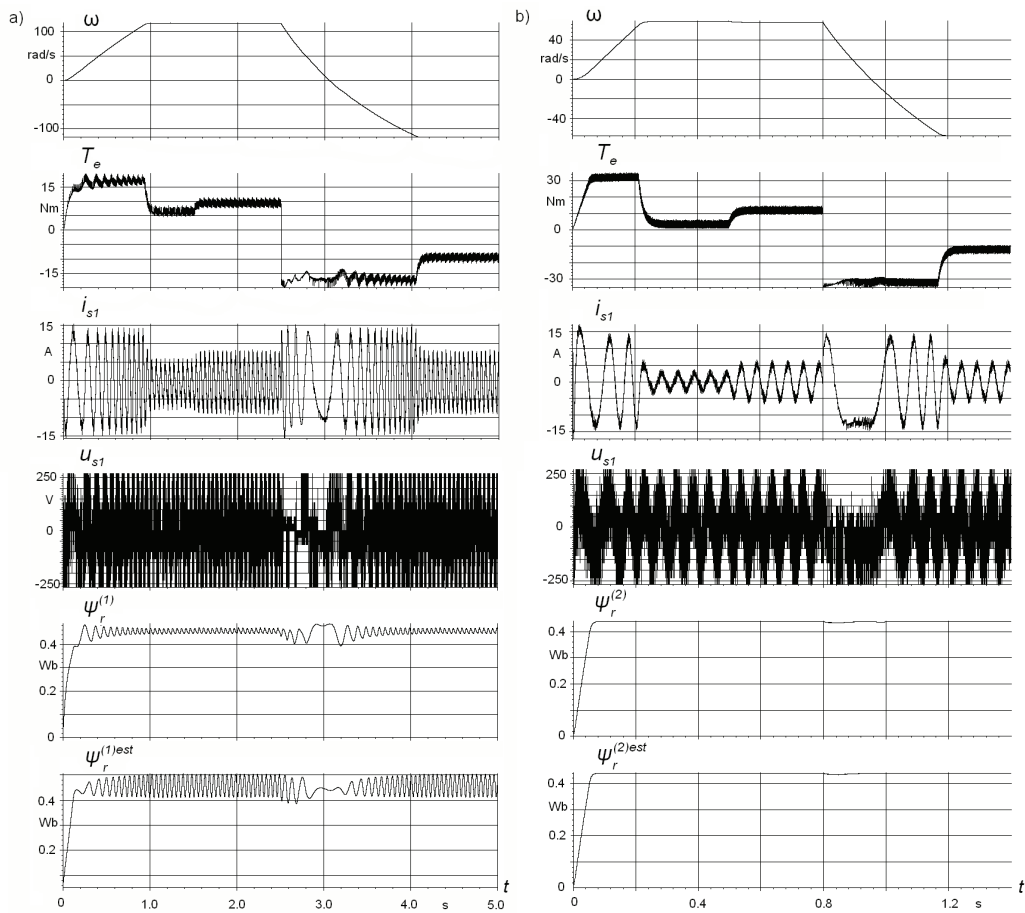


Fig. 6. Waveforms illustrating work of the drive for various  $m$  at varying loading torque of reactive type: a) for  $m = 1$ , b) for  $m = 2$

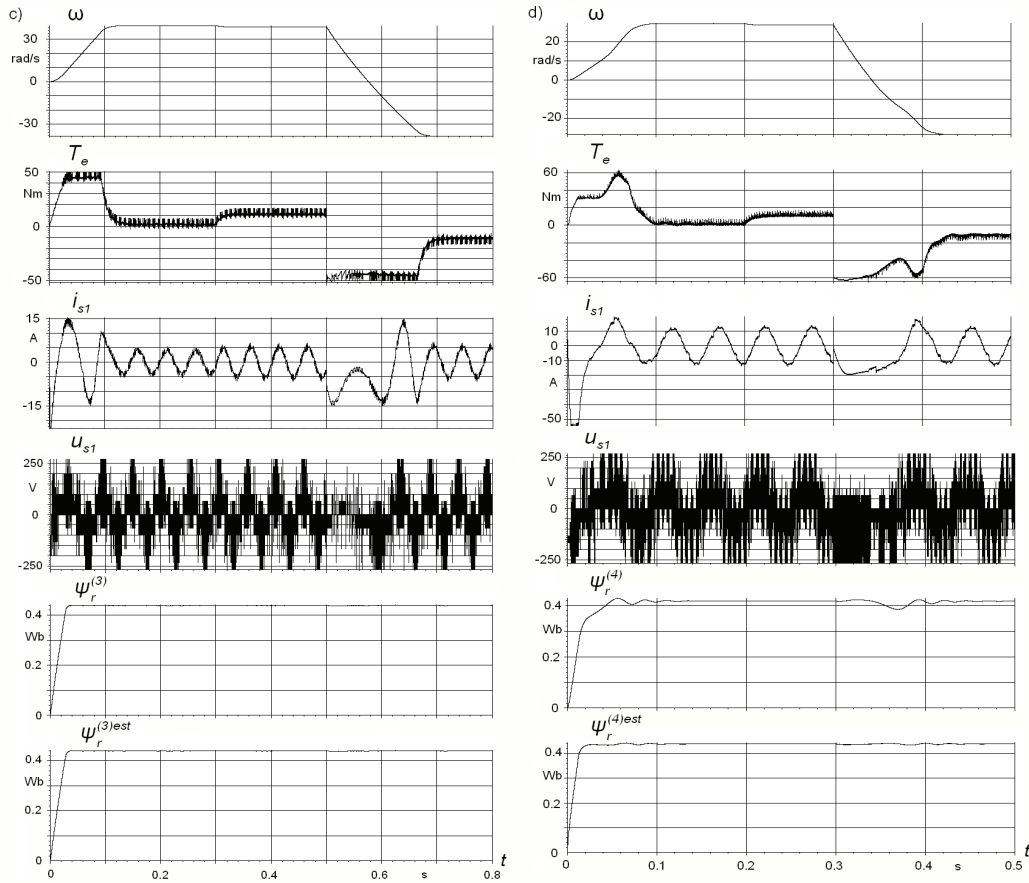


Fig. 6. Continuation for: c)  $m = 3$ , d)  $m = 4$

### 3.2. Examples of operation

For the studies the multiphase motor with the parameters  $M = 9$ ,  $N = 28$ ,  $S = 1$ ,  $p = 1$  was taken. The motor had a two-layer stator winding placed in 36 slots and divided into 9 four-coil phase windings of the first type. Stator phase winding resistance and its leakage inductance had values  $R_s = 1.2 \Omega$  and  $L_{\sigma s} = 11.3 \text{ mH}$  respectively. The magnetic core and the cage rotor were taken from the 4-pole, 3-phase motor Sf112M-4 (4.0 kW, 380 V, 50 Hz). The determined rated power of the 9-phase motor was  $P_N = 3.2 \text{ kW}$  for sinusoidal supply at  $m = 2$  and the voltage  $U_{sN} = 95 \text{ V r.m.s}$  (the same number of poles at  $m = 2$ ). Thus, the designed motor had a lower power with respect to the 3-phase one [10].

Operation of the 9-phase motor drive has been illustrated for starting, arise of loading and the speed reverse in Figures 6 and 7. The desired reference speed  $\omega^{\text{ref}} = 120/m \text{ rad/s}$  was settled as dependent on the sequence number  $m = 1, 2, 3, 4$ . The reference value for the rotor flux was constant  $\psi_r^{\text{ref}} = 0.45 \text{ Wb}$  for each  $m$ . The speed controller **R** $\omega$  was of  $P_{\text{sat}}$  type (proportional with saturation). At the saturation it was forcing a maximum value  $i_{sq\text{max}}^{(m)\text{ref}} = \pm 20 \text{ A}$

during speed transients for every  $m$ . This current component, together with the flux controlling component

$$i_{sd}^{(m)ref} = \frac{\Psi^{ref}}{L_{\mu}^{(m)}}$$

forces the greatest amplitude

$$I_{smax}^{(m)ref} = \frac{2}{\sqrt{M}} \sqrt{(i_{sd}^{(m)ref})^2 + (i_{sqmax}^{(m)ref})^2} \approx 15 \text{ A}$$

of phase current command signal for each sequence number  $m = 1, 2, 3, 4$ .

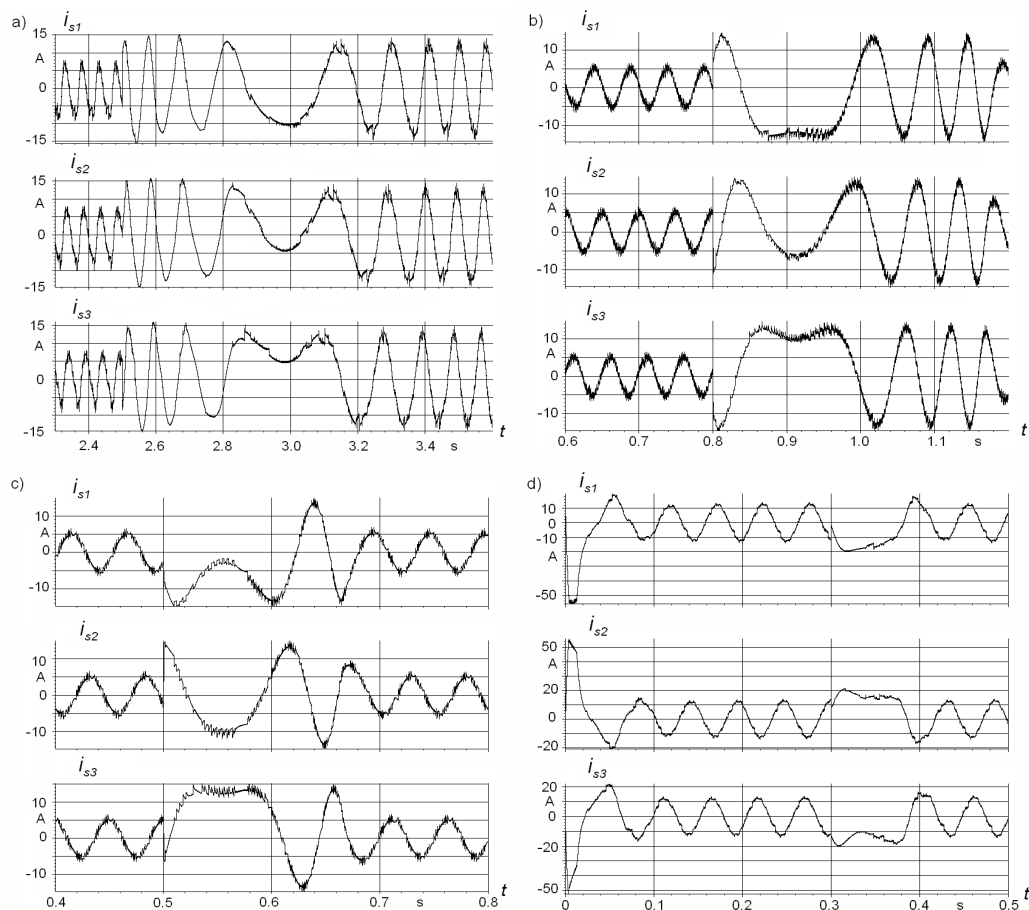


Fig. 7. Currents  $i_{s1}$ ,  $i_{s2}$ ,  $i_{s3}$  of the first three phases of the 9-phase motor for time interval of the motor reverse: a) for  $m = 1$ , b) for  $m = 2$ , c) for  $m = 3$ , d) for  $m = 4$

### 3.3. Comment

In Figure 6 the following waveforms are shown:  $\omega$  – motor angular speed,  $T_e$  – electromagnetic torque,  $i_{s1}$  – current of phase 1,  $u_{s1}$  – voltage induced in phase winding 1,  $\psi_r^{(m)}$  – mo-

dulus of rotor flux vector,  $\psi_r^{(m)\text{est}}$  – modulus of estimated rotor flux vector. The signal  $\psi_r^{(m)\text{est}}$  of estimated flux was determined in a simplified voltage model using signals after selection in **T3** (Fig. 5) according to (29). This signal was used for closed loop flux control in **R $\Psi$** .

In Figure 7 the waveforms of the first three phase currents for a given  $m$  are shown. These waveforms supplement the waveforms from Figure 6, however they are presented only for the time interval where the motor reverse becomes. Before the reverse the phase shift between the currents  $i_{sk}$  and  $i_{s(k+1)}$  is  $m\frac{2\pi}{9}$  and after the reverse this phase shift is  $(9-m)\frac{2\pi}{9}$  for each  $m = 1, 2, 3, 4$ . This shows the mutual change of supply sequence number from  $m$  for positive speed direction to  $M-m$  for inverse speed direction.

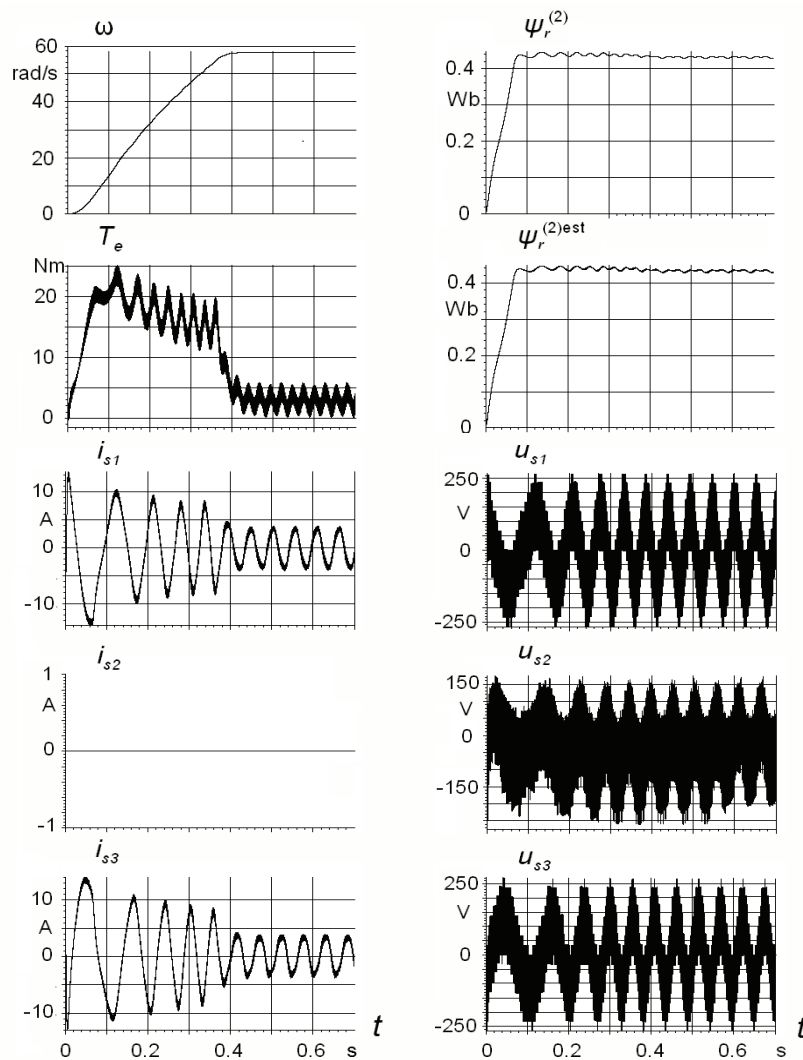


Fig. 8. Vector controlled 9-phase motor starting at a broken phase 2 for  $m = 2$ . The runs correspond to control conditions as for waveforms in Figure 6b

For a given  $m > 1$  the reference speed signals were  $m$  times lower than for  $m = 1$ , whereas the reference flux was the same. At dynamic states the produced electromagnetic torque was  $m$  times greater for the same current and flux than for  $m = 1$ . At dynamic states of starting, braking and reverse the torque was constant. So, the motor had the same power  $P_{\max} = \omega^{\text{ref}} T_{\text{emax}} = \omega^{\text{ref}} 2pm \psi^{\text{ref}} i_{sq}^{(m)\text{ref}} = 2160 \text{ W}$  for each  $m$ . It means that the change of  $m$  appears as a change of mechanical gear-box ratio from the point of view of transferred torque. However, the moment of inertia can not be reduced to the motor shaft as the mechanical gear-box does.

The controller  $\mathbf{R}\psi$  forces the rotor flux to the desired value  $\psi^{\text{ref}} = 0.45 \text{ Wb}$  the faster the greater is  $m$ , though some oscillations of the flux for  $m = 1$  appear influencing the electromagnetic torque. The drive operates stable for every  $m$ . Command signal  $i_{sd}^{(m)\text{ref}}$  increases for increasing  $m$ , since the inductance  $L_{\mu}^{(m)}$  is decreasing, whereas the flux reference signal  $\psi^{\text{ref}}$  is constant. This inductance depends directly on  $\nu = m$  and additionally on the winding factors – see (15). Increasing  $i_{sd}^{(m)\text{ref}}$  appears significantly for  $m = 4$ .

The speed control reacts similarly as for other drives. Quality of control depends mainly on type and parameters of  $\mathbf{R}\omega$ . The runs are typical for the  $P_{\text{sat}}$  controller where the stable control error at steady states is visible.

To illustrate the possibility of vector control at broken phase currents the waveforms for the motor starting at  $m = 2$  and  $i_{s2} = 0$  have been shown in Figure 8. Operation of the motor is worse than those depicted in Figure 6b, though the drive realises the demands. The voltage  $u_{s2}$  induced in the faulty phase has a different shape than the voltages of “healthy” phases. The results have been shown only for breaks caused by the inverter, whereas the open-circuited stator windings have a slightly different effect.

## 4. Conclusions

The drives with multiphase cage induction motors offer the following properties comparing to the 3-phase motor drives.

- Low speeds can be obtained at relatively high frequency and voltage for the supply sequence  $m > 1$ . A wide range of speed control can be realised at a voltage depth of modulation not lower than 0.45 for the motors with the first type of multiphase winding.
- The change of supply sequence gives the similar effect as the switched mechanical gear. However, this concerns only the torque and the supply sequence does not change the mechanical inertia according to the transmission ratio. The inverter can be designed for lower currents, since the greater torque (19) at lower speeds can be obtained due to greater  $m$  at the same current. This can find application in locomotive traction drives and ship propulsion where high dynamic torques are not demanded [6, 11, 12, 20, 24]. For electric cars the variable supply sequence brings profits due to the mentioned increase of electromagnetic torque.
- The motor can work with no more than  $(M - 3)$  open-circuited phases [4, 8, 10, 19]. This is important for fault-tolerant drives (high power industry drives, electric vehicle drives, ship propulsion).

- The control system forcing voltages would be more complicated than this presented in Figure 5, though it can be more universal having the possibility of switching to open loop control during so called “scalar control”.
- The control law presented in this paper has been based on the simplified two-phase motor model for all supply sequences  $m$  described by equations (16-20). So, for each  $m$  the motor is controlled in the same way. Similarly as for the 3-phase motors all sensor-less control methods can be trained as the applications for the multiphase motors. For example the MRAS speed estimator could be implemented in its standard form [16] or the improved one presented in [21]. The successful application of DTC was presented in [24], though considering a greater number of phases the optimal switching would be more difficult to define [19].
- The influence of supply sequence on the speed is possible due to interaction of space harmonics of magnetic field. So, the multiphase motor is an example where higher harmonics are useful. However, a strong parasitic interaction of higher harmonics can occur at the motor operation. To decrease this effect the stator winding of multiphase motors must be properly designed regarding the rotor cage [8, 10]. The motor with a sinusoidal winding has no such properties and the supply sequence does not influence the motor speed.
- Designing the multiphase motor with perfectly sinusoidal stator winding we obtain in practice the near-sinusoidal winding requiring more than one slot per pole per phase. This problem becomes more difficult when the number of phases increases. So, the power transferred from the stator to the motor shaft can usually be not greater than for the 3-phase motor of the same dimensions.

## References

- [1] Apsley J.M., Williamson S., *Analysis of multi-phase induction machines with winding faults*. Proc. IEEE IEMDC, San Antonio, TX, pp. 249-255 (2005).
- [2] Apsley J.M., Williamson S., Smith A.C., Barnes M., *Induction motor performance as a function of phase number*. Proc. Inst. Electr. Eng. Electr. Power Appl. 153(6): 898-904 (2006).
- [3] Atkinson G.J., Mecrow B.C., Jack A.G. et al., *The design of fault tolerant machines for aerospace applications*. Proc. IEEE IEMDC, San Antonio, TX, pp. 1863-1869 (2005).
- [4] De Silva P.S.N., Fletcher J.E., Williams B.W., *Analysis of concentrated winding multi-phase machines under phase failure using decoupled vector space theory*. Proc. IEE Int. Conf. PEMD, Dublin, Ireland, pp. 420-424 (2006).
- [5] Drozdowski P., *Equivalent circuit and performance characteristics of a 9-phase cage induction motor*. Int. Conf. on Electr. Machines ICEM'94, Paris (France) 1: 118-123 (1994).
- [6] Drozdowski P., *Some circumstances for an application of the 9-phase induction motor in the traction drive*. Second Int. Conf. “Modern Supply Systems and Drives for Electric Traction”, Warsaw, pp. 53-56 (1995).
- [7] Drozdowski P., *Field oriented control of a 9-phase cage induction motor*. Tech. Transactions (Czas. Tech.), Z.4-E/1998 Electrical Engineering, Wyd. PK, Kraków, pp. 1-25 (1998).
- [8] Drozdowski P., *Synthesis elements of polyphase windings for cage induction motors*. Archives of Electrical Engineering XLVIII(1-2): 63-68 (1999).
- [9] Drozdowski P., *A 9-phase cage induction motor fed by a  $3 \times 9$  matrix converter*. Proc. Int. Conf. on Electr. Machines ICEM'2000. Espoo (Finland) 1: 387-391 (2000).

- [10] Drozdowski P., *Shaping of duty characteristics and properties of polyphase cage induction motors* – in Polish. Cracow Univ. of Technology (Pol. Krak.) Monograph 278, Kraków, p. 255 (2000).
- [11] Drozdowski P., *Supply system for a 9-phase induction motor in electrical traction*. X Ogólnopolska Konf. Trakcji Elektrycznej, SEMTRAK 2004, Zakopane-Kościelisko 2004 (Poland), I: 191-198 (2004) (in Polish).
- [12] Drozdowski P., *Vehicle drive with a multiphase cage induction motor*. Tech. Transactions (Czas. Tech.). Wyd. PK, Kraków, 1-E(15): 49-60 (2009) (in Polish).
- [13] Drozdowski P., *Multiphase cage induction motors for controlled drives*. Zeszyty problemowe BOBRME KOMEL, Maszyny elektryczne. Katowice 2011, Int. Symposium on Electrical Machines, Szczecin, Poland 5(93): 7-12 (2011).
- [14] Figueroa J., Cros J., Viarouge P., *Generalized transformations for polyphase phase-modulation motors*. IEEE Trans. Energy Convers. 21(2): 332-341 (2006).
- [15] Fu J.R., Lipo T.A., *Disturbance-free operation of a multiphase current-regulated motor drive with an opened phase*. IEEE Trans. Ind. Appl. 30(5): 1267-1274 (1994).
- [16] Gadoue S.M., Abdel-Khalik A.S., *Speed Estimation performance for Multiphase Induction Machines under Fault Conditions*. Proceedings of the 14th International Middle East Power Systems Conference (MEPCON'10), Cairo University, Egypt, December 19-21, 2010, pp. 515-520.
- [17] Gritter D., Kalsi S.S., Henderson N., *Variable speed electric drive options for electric ships*. Proc. IEEE ESTS, Philadelphia, PA, 2005, pp. 347-354.
- [18] Levi E., Bojoi R., Profumo F. et al., *Multiphase induction motor drives – A technology status review*. IET Electr. Power Appl. 1(4): 489-516 (2007).
- [19] Levi E., *Multiphase electric machines for variable-speed applications*. IEEE Trans. on Industrial Electronics. 55(5): 1893-1909 (2008).
- [20] Mantero S., Monti A., Spreafico S., *DC-bus voltage control for double star asynchronous fed drive under fault conditions*. Proc. IEEE PESC, Galway, Ireland, pp. 533-538 (2000).
- [21] Orłowska-Kowalska T., Dybkowski M., *MRAS Speed estimators in the sensorless induction motor drive*. Power Electronics and Electrical Drives. Polish Academy of Sciences, Electrical Engineering Committee of Wyd. Pol. Wroc. Wrocław, pp. 223-241 (2007) (Poland).
- [22] Pereira L.A., Scharlau C.C., Pereira L.F.A., Haffner J.F., *General model of a five-phase induction machine allowing for harmonics in the air gap field*. IEEE Trans. on Energy Conversion 21(4): 891-899 (2006).
- [23] Pessina G., Zimaglia C., *Two speed commutated 5-phase induction motor*. Int. Conf. on Electr. Machines IECM'86 (Muenchen, Germany), Part 1: 199-202 (1986).
- [24] Shuai Lu., Corzine K., *Direct torque control of five-phase induction motor using space vector modulation with harmonics elimination and optimal switching sequence*. Applied Power Electr. Conf. and Exposition, 2006. APEC'06. 21 Annual IEEE, March 2006.
- [25] Sobczyk T.J., Weinreb K., *Steady state equations of multiphase squirrel-cage induction motors*. Int. Conf. on El. Machines IECM'86 (Muenchen, Germany), part 2: 393-396 (1986).
- [26] Sobczyk T.J., *Speed control of multiphase induction motors*. 34 Internation. Wissenschaftliche Koll. TH Ilmenau, pp. 145-148 (1989).
- [27] Steiner M., Deplazes R., Stemmler H., *A new transformerless topology for AC-fed traction vehicles using multi-star induction motors*. EPEJ 10(3/4): 45-53 (2000).
- [28] Teodorescu R., Tataru A.M., Lungeanu F., *Simulation of five-phase induction motor*. Proc. of 3<sup>rd</sup> Int. Symp. „Electromotion '99”. Patras (Greece), Paper A-13, 1: 93-96 (1999).
- [29] Terrien F., Siala S., Noy P., *Multiphase induction motor sensorless control for electric ship propulsion*. Proc. IEE PEMD Conf., Edinburgh, U.K., pp: 556-561 (2004).
- [30] Toliyat H.A., *Analysis and simulation of five-phase variable speed induction motor drives under asymmetrical connection*. IEEE Trans. on Power Electron. 13(4): 748-755 (1998).
- [31] Toliyat H.A., Lipo T.A., White J.C., *Analysis of a concentrated winding induction machine for adjustable speed drive applications. Part 1. Motor Analysis*. IEEE Trans. Energy Convers. 6(4): 679-683 (1991).
- [32] Toliyat H.A., Xu H., *A novel direct torque control (DTC) method for five-phase induction machines*. Proc. IEEE APEC, New Orleans, LA: 162-168 (2000).

- 
- [33] Xu H., Toliyat H.A., Petersen L.J., *Rotor field oriented control of five-phase induction motor with the combined fundamental and third harmonic currents*. Proc. IEEE APEC, Anaheim, CA, 2001, pp. 392-398.
- [34] Zhao Y., Lipo T.A., *Modeling and control of a multi-phase induction machine with structural unbalance*. IEEE Trans. on Energy Conv. 11(3): 570-584 (1996).